Applied Catalysis B: Environmental 168-169 (2015) 322–332

Contents lists available at ScienceDirect

Applied Catalysis B: Environmental

journal homepage: www.elsevier.com/locate/apcatb

Hydrotreating activity of bulk NiB alloy in model reaction of hydrodenitrogenation of carbazole

M. Lewandowski*

Centre of Polymer and Carbon Materials Marii Curie Skłodowskiej 34, 41-819 Zabrze, Poland

ARTICLE INFO

Article history:
Received 17 September 2014
Received in revised form
19 December 2014
Accepted 23 December 2014
Available online 27 December 2014

Keywords:
Bulk NiB alloy
Ni_3S_2
Hydrodenitrogenation (HDN) reaction
Carbazole
Hydrogenation
Metallic Ni^0

ABSTRACT

The separate and simultaneous (with hydrodesulfurization-HDS) hydrodenitrogenation (HDN) reactions of refractory model compound was performed over NiB bulk alloy. The model compound was carbazole. The catalysts were characterized by X-ray diffraction (XRD) before and after reactions, also by X-ray photoelectron spectroscopy (XPS), transmission electron microscopy (TEM) and scanning electron microscopy (SEM). The surface properties and texture of sample was determined by N_2 BET specific surface area and chemisorption of CO. For the alone HDN of carbazole this catalyst was very active in the whole range of applied contact times. For simultaneous HDN/HDS reactions activity of catalyst depressed due to competition reaction of HDS and partially sulfidation of catalyst. The main product of the HDN reaction (alone) was bicyclohexyl (BCH). It was also observed the consecutive reaction of isomerisation of the main product of the HDN reaction, BCH transformed mainly into ethylbicyclo[4,4,0]decane (EBC[4.4.0]decane) and also to hexylcyclohexane (C_6CH). During alone HDN reaction observed decompositions of NiB on metallic Ni and well dispersed boron. The alone reaction of HDN took place on metallic phase–Ni^0. Opposite for HDN reaction with HDS the consecutive reaction of isomerisation of the main product of the HDN was dominant – BCH transformed first of all into EBC[4.4.0]decane. During the HDN/HDS reaction observed partially formed Ni_3S_2, metallic Ni and Ni_3B. The activity was attributed first of all by presence of Ni^0 phase.

1. Introduction

The transition metal borides, particularly NiB and CoB alloys are well known as a good catalyst for hydrogenation reaction [1–7]. The process of hydrogenation is needed and widely used in production of fine chemicals, crude oil processing and many other areas. The interesting properties of borides (NiB and CoB) are its resistance for sulfur, compare to noble metals [8–10]. Luo et al. [8] studied adsorption of sulfur by means of the DFT method (density functional theory). Their theoretical conclusions have shown that sulfur prefers adding to boron, not to nickel alloy catalyst NiB. This allows for protection of active nickel against deactivation by sulfur during catalytic hydrogenation. The results by Luo et al. [8] have confirmed previous research by Li et al. [9] and Wang et al. [10] who state that sulfur in the NiB alloys adsorbs on the elementary boron in a reversible manner.

In the case of hydrodenitrogenation processes good hydrogenation activities of catalysts are necessary, since hydrogenation of aromatic rings with N-atoms is required before N removal. The amounts of sulfur and nitrogen compounds left after the first stage of hydrotreating expressed in S and N are 250–300 ppm in S and nearly 100 ppm in N [11].

Taking into account the aforementioned factors, namely: (i) resistance of transition metal borides to the presence of sulfur (role of boron), (ii) their hydrogenation activity necessary during deep hydrotreating process was included at the first stage of the research on their activity in a model HDN reaction of carbazole.

2. Experimental

2.1. Preparation of NiB alloy

The NiB amorphous alloy catalysts were prepared by the chemical reduction method. The solution of KBH_4 (2.0 mol/L) was used as the reducing agent. This solution was added drop-wisely to the solution of nickel salt ($NiCl_2$-0.1 mol/L) in room temperature and under N_2 atmosphere, during which the mixture was vigorously stirred. The resulting NiB alloy catalyst was washed with distilled

* Correspondence to: SYNTHOS S.A. Chemików 1, 32-600 Oświęcim, Poland, Building E-182. Tel.: +48 602 503 809.
E-mail address: marco297@wp.eu

http://dx.doi.org/10.1016/j.apcatb.2014.12.043
0926-3373/

water until its pH value was about 7 and then kept in ethanol absolute for future use.

2.2. Characterization

These materials were characterized by XRD, TEM, SEM, XPS, BET measurements and CO chemisorption, and elemental chemical analysis of nickel, boron (fresh catalyst) and carbon, hydrogen, nitrogen and sulfur (CHNS) after alone HDN and HDN/HDS reactions.

2.2.1. X-Ray Diffraction

Structural characterization of NiB catalyst before and after was carried out by X-ray diffraction (XRD) using a SIEMENS D-500 automatic diffractometer with the CuKα monochromatized radiation. The degrees of amorphous and crystallinity of the NiB alloy obtained were estimated from the intensity of all reflections in the range 2θ from 10° to 90°.

2.2.2. TEM, SEM analysis

TEM—transmission electron microscopy (TEM) was carried out on fresh and heated NiB alloy. The TEM study was performed using a FEI electron microscope model TF20-Tecnai G^2 200 KV.

SEM—scanning electron microscopy (SEM) was performance for NiB catalysts after HDS/HDN reactions. The SEM study was performed using a FEI electron microscope model Quanta FEG250.

2.2.3. XPS analysis

X-ray photoelectron spectroscopy (XPS) was performed on a Kratos AXIS 165 spectrometer with X-Ray Gun: mono Al Kα radiation ($h\nu$ = 1486.58 eV). For calibration the C 1s line at 284.8 eV was used as charge reference. Server and narrow regions spectra were acquired at pass energies of 160 eV and 20 eV respectively. Error in estimating bond energies was ±0.1 eV.

2.2.4. Specific surface area (SSA) measurements

Specific surface area was measured for the samples after reduction ex situ. The reduction was performed in the same conditions as in the reactor before catalytic test. The specific surface area (SSA) of the samples was determined from the N_2 adsorption isotherms at 77 K on an ASAP2010 apparatus (Micromeritics).

2.2.5. Dynamic CO titration–pulsed technique

CO uptake is a classical technique used to titrate the metallic sites. The CO uptake was performed "in situ" i.e., in the synthesis reactor without exposing the fresh NiB alloy to air or to the passivating mixture. Pulses of a known quantity of CO (17 μmol) were injected, at regular intervals, on the sample at RT in flowing He (40 mL min^{-1}) purified by an oxygen trap (Oxysorb, messer Griesheim). After each injection, the quantity of probe molecules not chemisorbed was measured using a conventional device equipped with a TCD. The injections were continued until CO saturated the surface. Data were processed and the number of micromoles of CO chemisorbed per gram of sample was determined.

2.2.6. Elemental chemical analysis

2.2.6.1. Nickel and boron. Elemental analysis for nickel and boron composition has been conducted with the ICP method with the ULTIMA 2 spectrometer. The sample was mineralized with the Multiwave 3000 mineralizer.

2.2.6.2. Carbon, hydrogen, nitrogen and sulfur. Elemental analysis of NiB alloy after the simultaneous HDS/HDN and HDN alone reactions were made by used FlashEA 2000 Thermo Scientific CHNS analyzer. The sample is weighed in tin capsules, placed inside the MAS 200R autosampler at a preset time, and then dropped into an oxidation/reduction reactor kept at a temperature of 900–1000 °C. The exact amount of oxygen required for optimum combustion of the sample is delivered into the combustion reactor at a precise time. The reaction of oxygen with the tin capsule at elevated temperature generates an exothermic reaction which raises the temperature to 1800 °C for a few seconds. At this high temperature both organic and inorganic substances are converted into elemental gases (CO_2, H_2O, SO_2, NO_x) which, after further reduction (NO_x to N_2), are separated in a chromatographic column and finally detected by a highly sensitive thermal conductivity detector (TCD).

2.3. Catalytic tests -hydrodenitrogenation

The simultaneous HDN/HDS and alone HDN was carried out with a down-flow fixed-bed microreactor in a high-pressure flow system. The catalyst (0.8 g for simultaneous HDN/HDS) was mixed with carborundum at the ratio of the catalyst to SiC = 1/5. For alone HDN reaction was took 0.2 g of catalyst. The liquid feed was fed to the reactor by means of a high-pressure piston pump through heated stainless tubes. The hydrogen flow (60–360 cm^3 min^{-1}) and total pressure were controlled by a mass flow controller and a back-pressure regulator, respectively. The temperature of the oven was regulated using a temperature controller.

The contact time (t_c) was defined as follows:

t_c (s) = catalyst volume (cm^3)/(H_2 flow + feed flow) (cm^3 s^{-1}).

The total conversion (conv.) of carbazole and degree of HDN of carbazole was defined following:

conv. of carbazole [%] = $\frac{N_N}{N_N+N_{carbazole}} \times 100\%$;

degree. of HDN [%] = $\frac{N_H}{N_N+N_{carbazole}} \times 100\%$where N_N is the sum of molar % of all products formed from after catalytic transformation of carbazole (including nitrogen containing compounds), $N_{carbazole}$ is the molar % of carbazole still present after reaction. N_H is the sum of molar % of all non nitrogen containing products formed after catalytic transformation of carbazole.

The liquid products of the reaction were collected every hour in the condenser whose temperature was maintained at 15 °C. Finally, this liquid was analyzed by gas chromatography (HP 4890) using a capillary column (HP1, 30 m × 0.25 mm × 0.25 μm) and a FID detector. The product identification was confirmed by GC/MS analysis with capillary column DB5, 30 m × 0.25 mm × 0.25 μm) and by electron-spray-ionization on Bruker–microTOF (ESI–TOF) instrument.

The HDN reaction of carbazole was performed separate and in the presence of sulfur compound (4,6-dimethyldibenzothiophene - 4,6-DMDBT) at 350 °C, under a total pressure of 6.0 MPa with a molar H_2/feed ratio of 600. The liquid feed contained 0.08% carbazole (100 ppm N) or 0.08% carbazole and 0.17% 4,6-DMDBT (300 ppm S) in o-xylene. Before starting the catalytic tests, each catalyst was heating in situ at 623 K (350 °C) for 2 h in pure dihydrogen atmosphere. The catalytic process was conducted for about 100 h. After about 100 h, the initial operating conditions were reset in order to check again the activity of the catalyst. The conversion of solvent was checked over all catalyst. It was observed that practically no conversion of the solvent took place in the operating conditions. The catalysts after reactions were kept in solvent–o-xylene for further characterization.

3. Results

3.1. CO chemisorption

The experimental CO uptakes of the sample of bulk NiB alloy (after heated 350 °C 6 h in presence of H_2 atmosphere in situ) was 109.3 μmol g^{-1}. The stoichiometry factor for CO chemisorptions

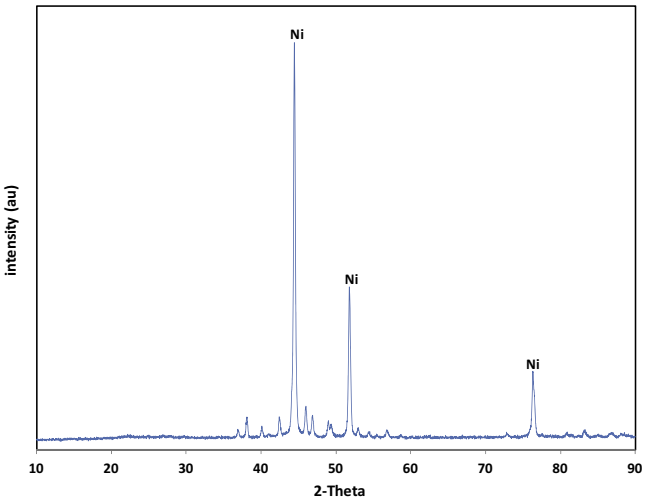

Fig. 1. XRD pattern of catalyst after heated in H_2 at 350 °C.

on Ni metal is 2. Therefore, as calculated there is 54.7 μmol of Ni atoms per gram on the surface of the bulk NiB alloy, which is equal to 8.48×10^{17} atoms of Ni per 1 m^2 of catalyst surface. The additional measurements of chemisorptions of CO after the HDN and HDN/HDS reactions were carried out. After the HDN reaction the quantity of chemisorbed CO decreased from 109.3 μmol/g to 78.4 μmol/g, while for the catalyst after HDN/HDS reaction it decreased to 37.4 μmol/g.

3.2. Specific surface area

The specific surface area of the NiB alloy catalysts was 38.8 m^2/g. After catalytic test specific surface areas decreased to value 11.7 m^2/g (after alone HDN) and about 10.5 m^2/g (after simultaneous HDN/HDS reactions). The mean reason is due to crystallization of samples during the reaction (influence of temperature).

3.3. XRD diffraction

Fig. 1 shows the XRD pattern of NiB catalyst heated in H_2 at 350 °C for 2 h, under atmospheric pressure (the same was done "in situ" in reactor, but under high pressure of H_2).

In Fig. 1 three main peaks correspond to metallic Ni^0 (JCPDS #01-071-3740) and the remaining, much smaller peaks correspond to Ni_3B phase (JCPDS #01-073-1792).

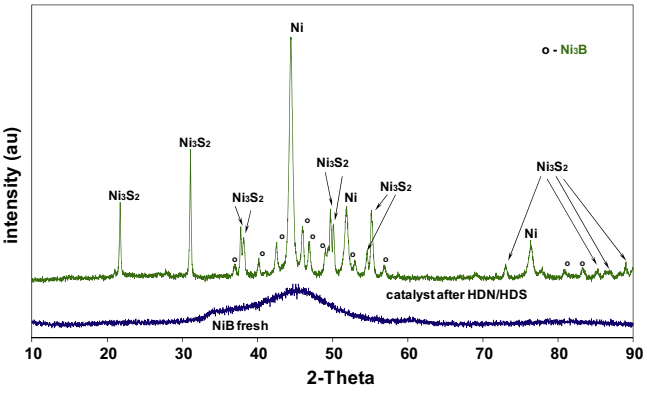

Fig. 2. X-ray diffraction patterns of fresh NiB alloy and catalyst after simultaneous HDN/HDS reactions.

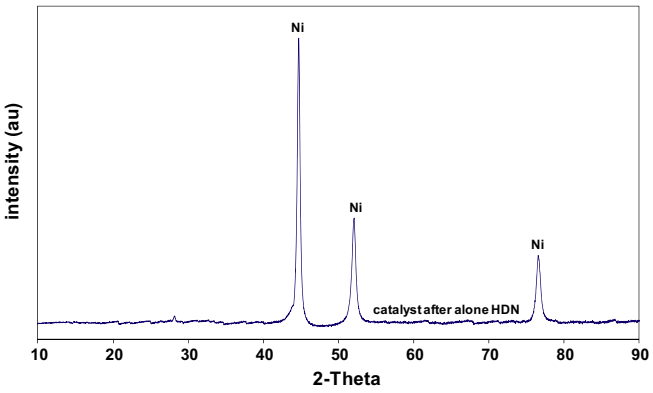

Fig. 3. X-ray diffraction patterns of bulk catalyst after alone HDN reaction.

Fig. 2 shows diffraction patterns of bulk NiB alloy catalyst (fresh) and catalyst following HDN/HDS reactions.

In the XRD pattern of NiB catalyst following 'fresh' synthesis (Fig. 2) only a broad peak is visible for $2\theta = 45°$. This peak is typical of NiB alloy amorphous structure [12]. However, pattern of the catalyst sample after the HDN/HDS is exceedingly different. This pattern features presence of new, relatively large peaks, mainly for $2\theta =$ 21.75° and 31.10°, as well as a few smaller ones (marked on Fig. 2) which are characteristic of Ni_3S_2 crystallographic phase (JCPDS #00-030-0863) corresponding to low-temperature structure of Ni_3S_2 sulfide of heazlewoodlite-phase type [13]. The remaining peaks present in the pattern are related to the presence of both metallic Ni (JCPDS #01-071-3740) and Ni_3B phase (JCPDS #01-073-1792). This shows that either crystallization or partial decomposition of the NiB alloy – both connected with the temperature of reaction – took place along with the catalyst sulfidation. The presence of the Ni and Ni_3B phase proves that the sulfidation process which proceeds during the HDN/HDS simultaneous reaction is incomplete.

Moreover, Fig. 3 presents the XRD pattern of the NiB sample after the carbazole HDN alone. The pattern features only three clear, high-intense peaks characteristic of metallic Ni^0 (JCPDS #01-071-3740). Similar observation was made by Chen et al. [14] on the XRD pattern. After heat- treatment of the alloy before the reaction, the real catalyst is the metallic Ni^0 in environment of highly dispersed boron species ($B + B_2O_3$) and very small amount Ni_3B phase – Fig. 1. Probably after preheating "in situ" and first two hours of reaction the Ni_3B phase decomposes completely to Ni and B and active phase is metallic nickel. We can say, that NiB alloy is in fact a precursor of real catalyst, which is metallic Ni^0 in environment of boron species–bulk catalyst.

3.4. Elemental analysis

Quantitative composition of the preparation obtained after elemental analysis was the following: 87.2% of nickel and 7.1% of boron, which corresponded to the stoichiometric ratio Ni to B = 2.3:1. The molar ratio of nickel to boron in the NiB preparation nearly equals 2 to 1 and is characteristic of this kind of prepared systems [15,16].

Based on this analysis, it was concluded that Ni + B constitutes 94.3%, so the remaining 5.7% is oxygen in form of B_2O_3. Similar was observed by Wang, et al. [17] and Li et al. [18]. Moreover the formation of large amounts of boron oxides in the process of the alloy production is considered unavoidable [9,19].

Based on ICP results it can be concluded that 36.6% of boron exists in form of B_2O_3. Formation of the boron oxide insted of NiO is termodynamically favourable because the former has a free energy

Table 1

NiB catalyst	N [ppm]	C [%]	H [%]	S [%]
HDN	1268	4.4	2.02	0
HDN/HDS	713	0.85	0.88	8.33

of formation (ΔG) of −801 KJ/mol O_2, whereas the latter has a ΔG value −426 KJ/mol O_2 [20].

Therefore the "fresh" catalysts is composed of highly dispersed B species in NiB alloy and amorphous states of both B_2O_3 and B [17], which is also observed after heat treatment at 350 °C in hydrogen and after reaction of alone HDN– Figs. 1 and 3.

Results of the elemental analysis of samples after HDN alone and the simultaneous HDN/HDS reactions were presence in Table 1:

On the base of this elemental analysis we can say (after calculated), that only about 27% of Ni was transformed into Ni_3S_2 during the simultanously HDS/HDN reactions. Amounts of nitrogen, carbon and hydrogen are different compare to analysis after HDN/HDS. No detected sulfur because it was reaction without HDS of 4,6-DMDBT.

3.5. SEM and TEM analysis

SEM morphology of bulk NiB catalyst after alone HDN of carbazole is present in Fig. 4 together with EDS analysis. The morphology is cotton-like structure. It is more clearly in image with bigger zoom– Fig. 4b. EDS analysis is detected first of all nickel with very small amount of carbon. No observed peaks responsible to nitrogen. It is agreements with elemental analysis. According the XRD analysis we can say that sample after alone HDN reaction is crystalline. We can not see it in SEM image. Probably the crystals are too small.

Note that interpretation of TEM image (Fig. 5) data is difficult, because the detailed structure of the nickel is not conspicuously clear, but we can see the fringes on the image becomes from small polycrystalline structure.

3.6. X-ray photoelectron spectroscopy (XPS)

Fig. 6 shows XPS spectra of the studied catalyst including Ni $2p_{3/2}$, O 1s, B 1s and S 2p lines together with quantification from survey spectra (atomic %) of the surface of the catalyst after (A) alone and (B) simultaneous HDN/HDS reactions. Fig. 7 shows the Ni $2p_{3/2}$ XPS spectra with four peaks at binding energies of 852.6 eV, 853.9 eV, 856.7 eV and 861.8 eV respectively after deconvolution. The curve A corresponds to the XPS spectra of the catalyst after the process of carbazole HDN alone. The first peak (852.6 eV) in Ni $2p_{3/2}$ level is assigned to metallic nickel (Ni^0) [17,19,21]. The second main peak (856.9 eV-satellite peak) is attributed a presence of oxidized nickel (NiO) [19] The remaining peak (853.9 eV) in Ni $2p_{3/2}$ level is assigned to the Ni present in the NiB alloy. The Ni $2p_{3/2}$ binding energies for the borides are slightly higher than that for Ni^0 [19]. The associated satellite peak near 862.1 eV indicates the presence more than one "nickel–oxygen" species on the surface of catalyst. The "nicke–oxygen" species on surface are observed due to surface oxidation during the pasivation and removal of catalyst from the reactor and separation from SiC with the inevitable contact with air

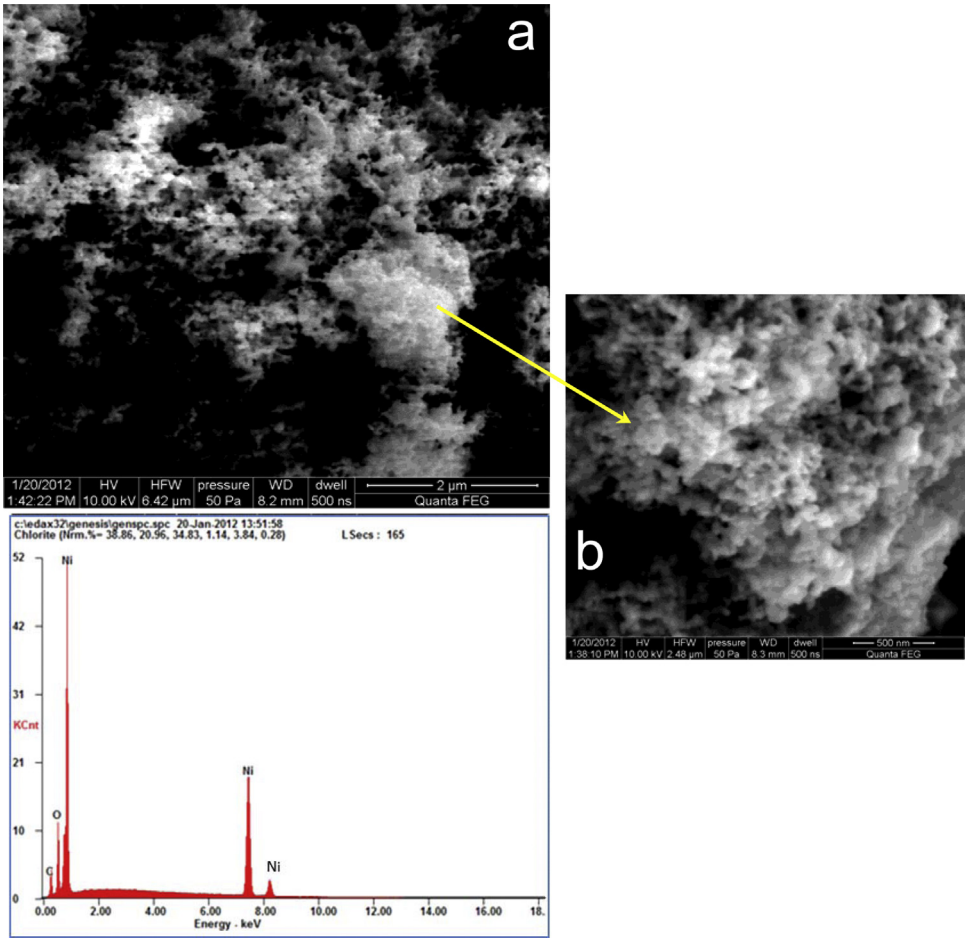

Fig. 4. SEM morphology with EDS analysis for bulk catalyst after alone HDN of carbazole.

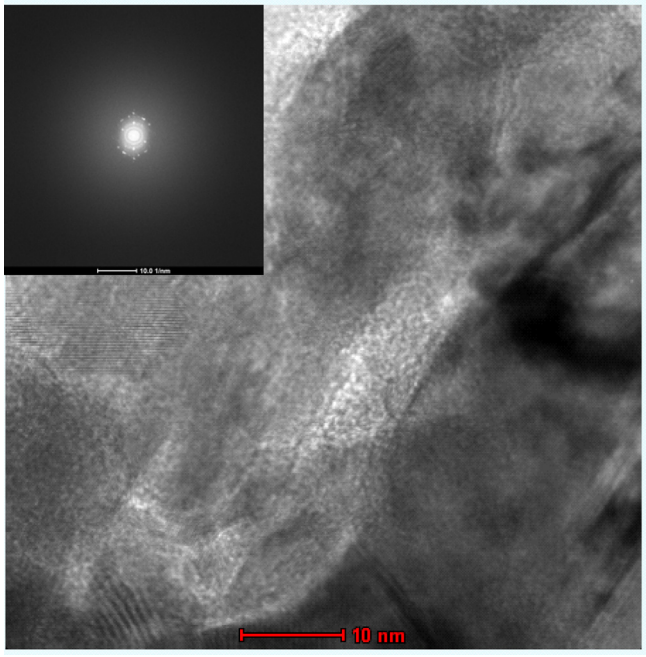

Fig. 5. TEM images of bulk catalyst after alone HDN of carbazole.

before storage in solvent o-xylene. XPS results are in accordance with the results of XRD - only stated to the presence of metallic nickel in bulk structure of catalyst after HDN of carbazole. XPS spectrum of the same catalyst but after HDN/HDS process (Fig. 7B) is similar to the XPS spectra only after the process of HDN alone. In fact the difference is in intensity of peak with binding energy 852.6 eV. Necessary to emphasize that for Ni_3S_2 $Ni(2p)_{3/2}$ binding energy is close to the of nickel metal [22]. So can say that the intensity of the peak of the binding energy of 852.6 eV is the total intensity associated with the presence of metallic nickel and associated Ni_3S_2. Moreover, summary of quantification of high resolution spectra of only interested elements (Ni, S, B) shows, that still 30% of the surface nickel atoms exist as Ni^0 – it means not connected as a Ni_3S_2.

Fig. 8 shows two well resolved sulfur peaks at 162.4 eV and 163.3 eV corresponding to $S2p_{3/2}$ and $S2p_{1/2}$ respectively, typical for Ni_3S_2 [23–26]. These results confirm presence of Ni_3S_2 crystallites as detected by XRD analysis, these crystallites are formed during the HDN/HDS simultaneously reaction.

The B 1s spectrum presented in Fig. 9 contains only one peak near 193.2 eV for both reactions, which corresponds to oxidized boron [2,27,28]. This value is far from the value obtained for pure B (186.7 eV). Only one peak is observed, due to surface oxidation during the removal of catalyst from the reactor and separation from SiC resulting from inevitable contact with air before storage in solvent–o-xylene.

Fig. 10 shows the spectra XPS C 1s (carbon deposit) of catalysts after both reactions-HDN alone and HDN/HDS. In both cases the binding energy (BE) of 285.1 eV indicates the presence of carbon C_{sp3} (C—C) on the catalysts surface [29,30].

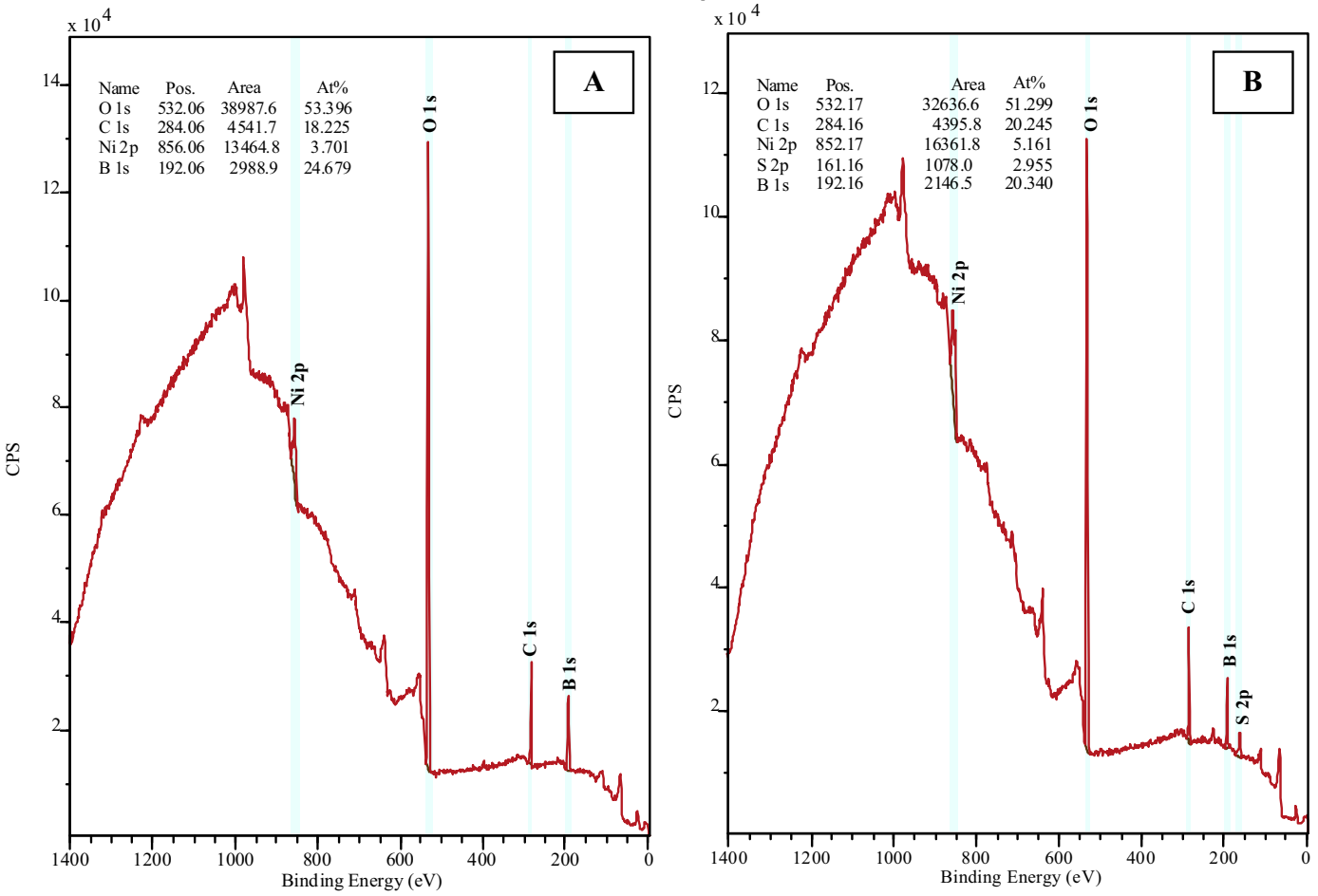

Fig. 6. Survey XPS spectra of NiB catalysts (A) after HDN alone and (B) after HDN/HDS reaction.

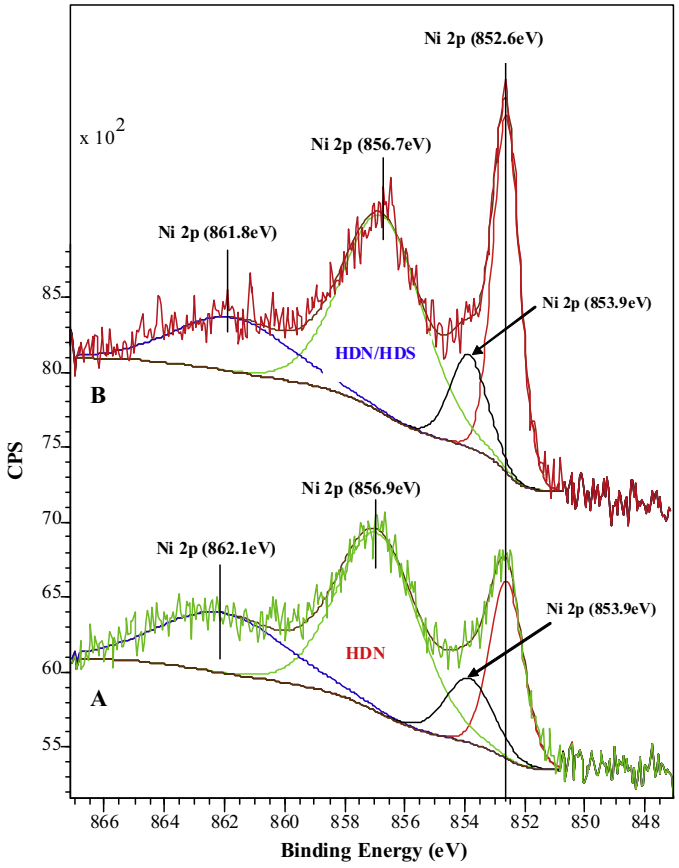

Fig. 7. Ni $2p_{2/3}$ XPS spectra of surface of bulk catalyst (A) - HDN alone reaction, (B) - after HDN/HDS reaction.

3.7. Hydrodenitrogenation

Fig. 11 depicts relation between conversion and the degree of hydrodenitrogenation since the contact time for the HDN reaction of carbazole with and without the simultaneous HDS 4,6-DMDBT reaction.

In carbazole HDN alone, the bulk catalyst was highly active. For the short contact times $t_c < 0.23$ s there was a high difference between conversion and the degree of hydrodenitrogenation of carbazole, which was caused by formation of tetrahydrocarbazole (THC) in large amounts. For the longest contact time $t_c = 0.68$s, the HDN reaction was practically complete – 100% of hydrodenitrogenation was obtained.

For the HDN reaction of carbazole along with HDS 4,6-DMDBT, the reason for the range of the time contacts used (contact times were about three times longer) was determined by obtaining wide range of conversion of a model compound which was comparable to the range of conversion in the carbazole HDN reaction alone. In this case it was also observed that for the shorter contact times $t_c < 0.73$ s there was a clear difference between the conversion of carbazole and its degree of hydrodenitrogenation.

Figs. 12 and 13 present product distributions of carbazole HDN alone and along with HDS respectively. The HDN reaction of carbazole on the bulk catalyst proceeds through carbazole hydrogenation into a reaction intermediate which is tetrahydrocarbazole (THC), and the major product of HDN is bicyclohexyl (BCH). Moreover, the presence of ethylbicyclo[4,4,0]decane (EBC[4.4.0]decane) and *n*-hexylcyclohexane (C_6CH) was confirmed. For the HDN reaction alone (Fig. 12), the amount of THC goes through relatively maximum yield of about 26% for $t_c = 0.11$ s. Therefore, it may be stated that under these conditions it is dominant along with BCH. Formation of small amount (<3%) of cyclohexylbenzene (CHB) was also observed. For the longer contact times $t_c > 0.11$ s there is a rapid decrease of the amount of the THC obtained, and the amount of CHB is reduced to zero. It may be assumed that under conditions of the applied contact times $t_c \leq 0.17$ s (Fig. 12) the reaction rate of HDN of carbazole is limited by the reaction rate of THC into HDN products, mainly BCH. For the longer contact times $t_c \geq 0.23$ s, conversion of THC becomes a stage which does not limit the total reaction rate since, as mentioned before, its amount is practically reduced to zero. For $t_c > 0.34$ s, only BCH and its isomers EBC[4.4.0]decane and C_6CH are present among the reaction products. However, BCH is decidedly dominant. For $t_c \geq 0.23$s the amount of EBC[4.4.0]decane is practically constant, independently of the contact time. For $t = 0.68$ s and with carbazole 100% reacted, the major reaction products are 62% of BCH and its isomers–EBC[4.4.0]decane (29%) and C_6CH (9%). On the basis of the results (Fig. 12), it may be stated that the resultant CHB (although formed in small amounts) at longer contact times ($t_c \geq 0.23$ s) undergoes hydrogenation into BCH since, as mentioned before, its amount is reduced to 0%. In the case of HDN of carbazole ran simultaneously with HDS (Fig. 13), BCH was not the dominant reaction product but so were products of its isomerisation. Also in this case the HDN reaction proceeds through THC formation (formed in a relatively large amount as well) at the maximum yield of about 20% for $t_c = 0.37$ s. For this contact time it constituted the major reaction product. When the contact time was increasing, the amount of THC was consistently decreasing, and mostly EBC[4.4.0]decane was significantly increasing. Also the amount of the resultant CHB was low (2–3%), and at the longest contact time it decreased to zero. Thus, as suggested in the case of the HDN reaction alone, eventually CHB underwent hydrogenation into BCH. Obviously in both cases this reaction path with CHB formed is practically marginal.

Generally, HDN of carbazole on the real bulk catalyst proceeds identically in both cases. It shows on Scheme 1. During HDN of carbazole a consecutive isomerisation of the hydrogenation product–BCH–took place. The consecutive isomerisation is prevalent for the simultaneous HDN of carbazole ran along with HDS 4,6-DMDBT (Fig. 13) –however this refers to the contact times three times as long as the contact times of carbazole HDN alone.

The key difference is seen in the yield of the reaction products. The major product of carbazole HDN alone was BCH and lower amount of its isomers (Fig. 12). However in the latter case (HDN along with HDS– Fig. 13) the number of isomers was dominant–mainly EBC[4.4.0]decane. Therefore, at the simultaneous HDS/HDN the consecutive isomerisation of HDN product was the leading reaction. When 4.6-DMDBT is present in feed mixture the selectivity of BCH is decreasing from about 62 to about 22 molar%, while the selectivity of both its isomers (EBC[4.4.0]decane + C_6CH) is increasing from about 34 to 74 molar%.

The commercial bulk alloy NiB was no active in HDN of carbazole in applied conditions – because of highly crystalline - a very small surface area of about 2 m^2.

3.8. Stabilization of catalysts

The stabilization of NiB alloy for conversions of carbazole in alone and the simultaneous reactions of HDN/HDS versus the time on stream is presented in Fig. 14. The catalytic process was conducted for about 100 h. After this time the initial conditions of the reaction were reset (initial contact time) and the reaction was continued to obtained stable catalytic activity again (after about additional 10 h). Since, the activity returned practically to the initial level for HDN reaction–alone and simultaneously (for longest contact time). In both cases of HDN reaction of carbazole the reaction practically is over (100%). For shorter contact times ($t_c \leq 1.10$ s for HDN/HDS and ≤ 0.34 s for HDN alone) the difference is larger

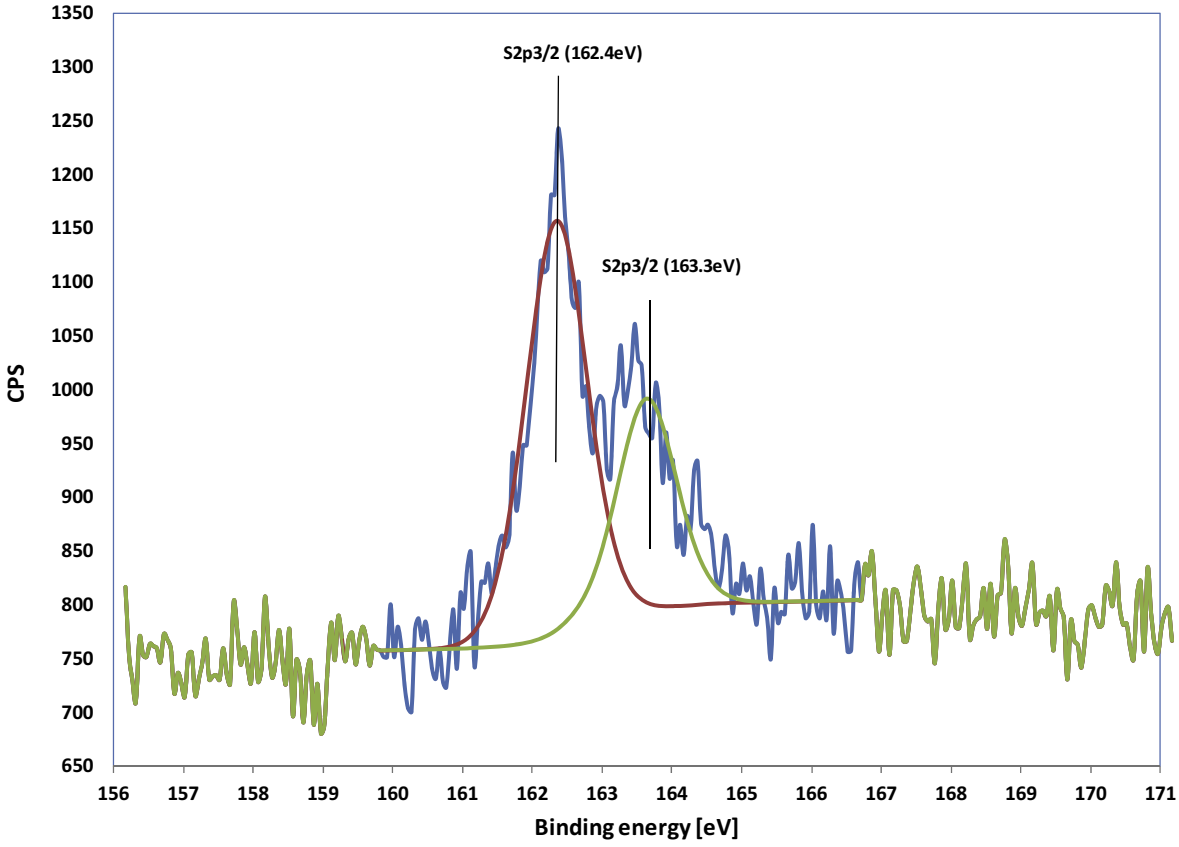

Fig. 8. S 2p XPS spectra of surface of bulk catalyst after HDN/HDS reaction.

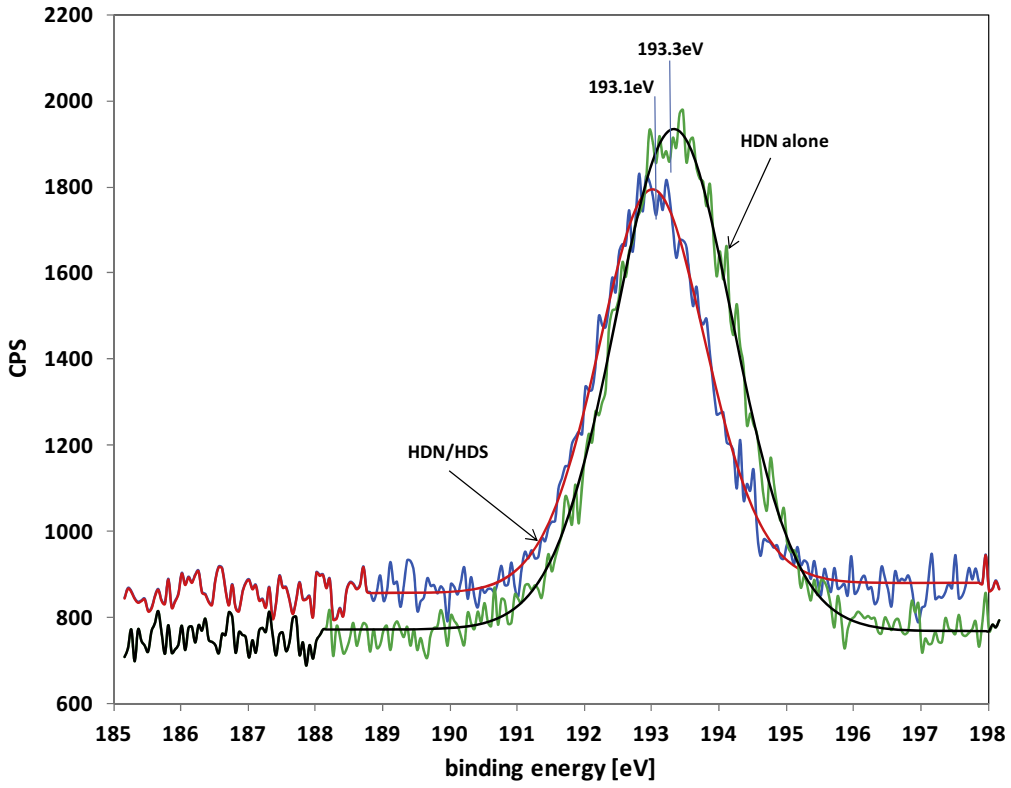

Fig. 9. B 1s XPS spectra of surface of bulk catalyst after HDN alone and HDN/HDS reactions.

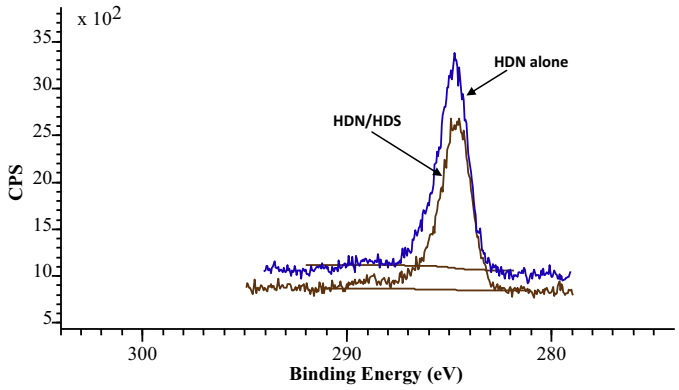

Fig. 10. C 1s XPS spectra of surface of bulk catalyst after HDN alone and HDN/HDS reactions.

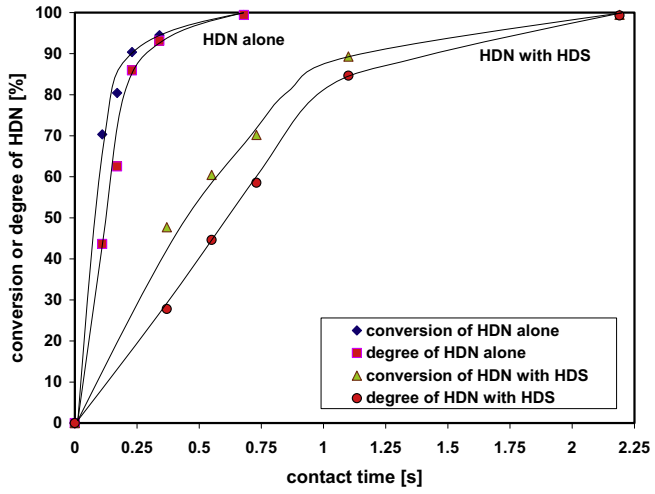

Fig. 11. Conversion and degree of HDN vs. contact time over NiB alloy –HDN reaction alone and together with HDS of 4,6-DMDBT.

and is in the range of 17–23% - due to competition HDS reaction of 4.6-DMDBT and partially sulfidation of catalysts. In the case of 20%Ni/SiO_2 catalyst (reference catalysts – results not presented here) decrease of the conversion of about 18% was observed, if compared to about 2% for our catalyst tested under the same procedure and reaction condition – for HDN/HDS reactions.

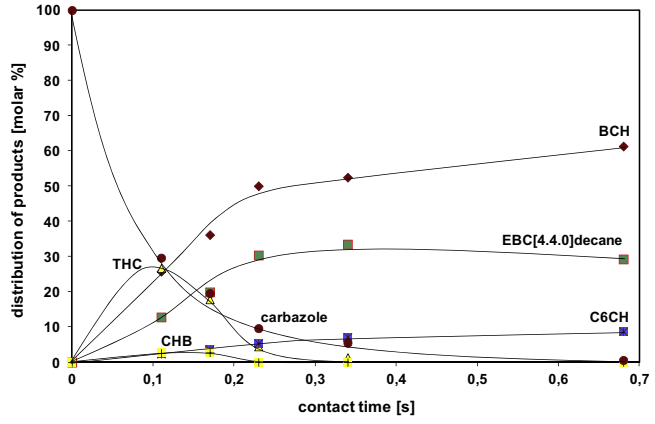

Fig. 12. Products distribution for the HDN of carbazole over bulk catalyst - alone HDN reaction.

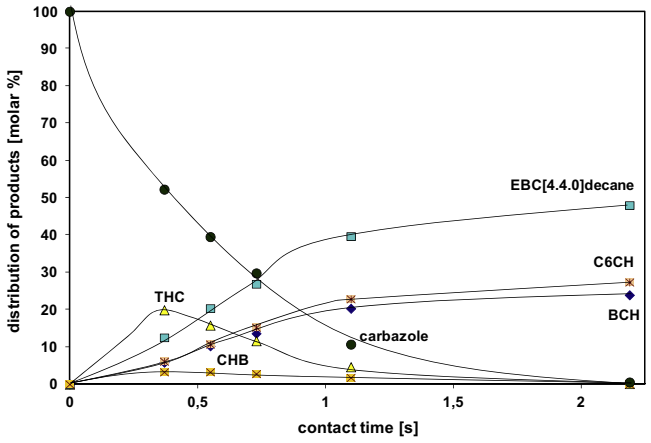

Fig. 13. Products distribution for the HDN of carbazole over bulk catalyst - HDN reaction together with HDS of 4,6-DMDBT.

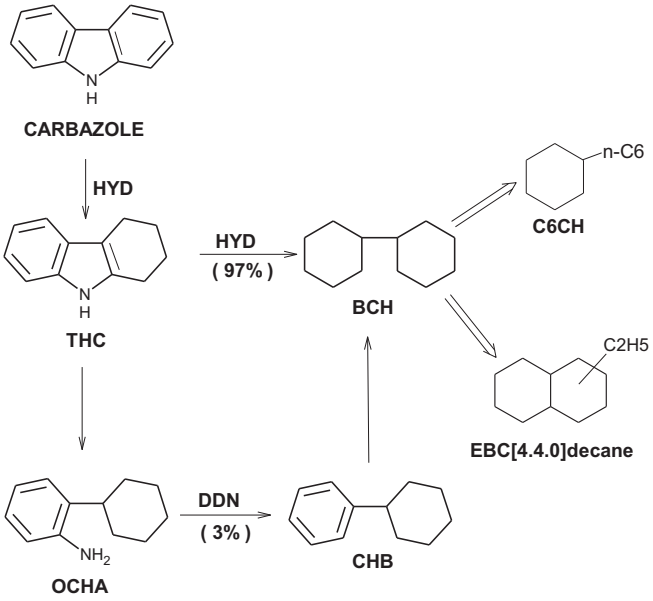

Scheme 1. Reaction pathways of the HDN of carbazole over bulk NiB alloy.

4. Discussion

4.1. XRD

The XRD results show that the broad peak present at $2\theta = 45^\circ$ corresponds to structure of the NiB alloy [18,31,32]– Fig.2.

However, in the XRD pattern of catalyst after HDN/HDS (Fig. 2) appear peaks assigned to the resultant Ni (JCPDS #01-071-3740), Ni_3B (JCPDS #01-073-1792) and Ni_3S_2 (JCPDS #00-030-0863). Therefore, it may stated that partial sulfidation of catalyst proceeds during the catalytic test. Yet apart from the sulfide phase (sulfidation), metallic Ni and crystallites Ni_3B are still present and are responsible for the catalyst being active. Thus, in this case the system includes Ni, Ni_3S_2, Ni_3B and B which is not visible in the XRD pattern due to its relatively low amount and good dispersion [33]. Skrabalak and Suslick [34] also confirmed thermal instability of the bulk Ni(Co)B under sulfidation conditions (450°C i 10% H_2S/H_2), however a part of the boride phase was still present in the catalyst, which our study has shown (Ni_3B) as well.

Fig. 3 depicts pattern of the catalyst after carbazole HDN alone. In the pattern, there are only three peaks clearly visible and assigned to the metallic nickel (JCPDS #01-071-3740). Therefore it may

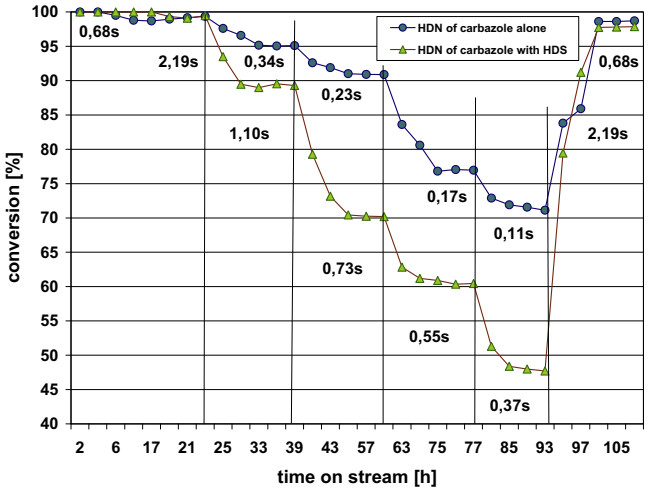

Fig. 14. Stabilization of conversion for NiB alloy catalyst versus time on stream for HDN of carbazole reactions alone and together with HDS. The range of contact time: 0.11 s–0.68 s for alone HDN, and 0.37 s–2.19 s for HDN with HDS.

be stated that during preheating and first 2–3 h of HDN of carbazole only decomposition of the NiB alloy into metallic nickel and dispersed boron species takes place, which is related to the influence the reaction temperature has on the NiB alloy decomposition [18,33].

It is well described in the literature that in NiB alloy, boron and boron oxide are very well dispersed, even during heating at high temperatures [17,18]. Lack of peaks characteristic for crystalline phase B and B_2O_3, as show in XRD pattern of catalyst after HDN alone (Fig. 3) and after heating at 350°C - Fig. 1, confirm that B and B_2O_3 are well dispersed. The increase in temperature induces crystallisation of the amorphous alloy and its segregation. The alloys are thermodynamically unstable and show a tendency to crystallisation at higher temperatures [18]. At lower temperatures the sample crystallises in the form of Ni_2B and Ni_3B, while at higher temperatures on the surface of the sample free metal and boron appear [18]. Wei et al. [35] have also proved the formation of Ni nanocrystallites and Ni_3B crystallites by the method of XAFS. All of these literature confirms our results. Moreover, the crystallisation can take place also as a result of a long-term storage at an elevated temperature (time of stream) [36] which leads to complete decomposition of the alloy to metallic Ni and highly dispersed boron species ($B + B_2O_3$) [18], as it is shown in Fig. 3.

4.2. Hydrodenitrogenation

In comparison with hydrodesulfurisation for example DBT, direct denitrogenation of carbazole is not observed due to the different nature of both molecules. The molecule of carbazole is more aromatic, than DBT. The free electrons pair of nitrogen is involved in electron resonance of the middle ring and therefore are not available for interaction with the catalyst surface [37,38]. This causes that the preferred adsorption through the π-electrons of the aromatic ring, which makes the hydrogenation easier. To remove N atoms from heterocyclic N-compounds, the scission C—N bond is fundamental step. Depending on the kind of C—N bonds, there are two types: $C_{(sp2)}$—N (unsaturated heterocyclic or aromatic amines) and $C_{(sp3)}$—N (saturated heterocyclic and non-aromatic amines). Thus, complete saturation of N-aromatic ring is necessary to scission $C_{(sp2)}$—N bond before nitrogen atom is removed via $C_{(sp3)}$—N bond cleavage (less $C_{(sp3)}$—N bond energy that for $C_{(sp2)}$—N). It mean, that hydrogenation of aromatic ring with N atom is kinetically the very important step in HDN [11]. HDN of carbazole with and without the simultaneous HDS 4,6-DMDBT reaction proceeded in a very similar way resulting in BCH [39–42] as the major product and low amounts of CHB (which disappears at longer contact times). In carbazole HDN alone (Fig. 12) the examined our catalyst was highly active. It may be assumed that its high activity was related to the presence of metallic nickel displaying hydrogenation and hydrogenolysis properties [6,7] necessary for the HDN reaction.

The major product of HDN of carbazole was BCH (Fig. 12). Moreover, relatively large amounts of BCH isomers were observed, namely C_6CH and EBC[4.4.0]decane (mostly) [39,42], which indicates presence of consecutive isomerisation of the HDN products. Yet the amount of isomers (EBC[4.4.0]decane and C_6CH) is considerably lower than in the case of the resultant BCH. However, it may be stated that carbazole HDN alone (as mentioned before) proceeds on the Ni metallic phase of the catalyst, since only the presence of metallic Ni on the catalyst was found following the HDN reaction (XRD pattern– Fig. 3). We can say: (i) that the catalyst transformation of the initial NiB material should occur in the flowing HDN feed very early and therefore there is the same catalyst during the full time on run; (ii) XRD patterns shows the true working catalysts during the full time on stream after HDN. The working catalyst for HDN alone may be formed during the pre-treatment and first few hours and it is quite stable.

Different situation takes place for HDN/HDS reaction (Fig. 13). Obviously, the type of the resultant products is the same, yet the consecutive isomerisation of BCH into EBC[4.4.0]decane and C_6CH is the prevalent reaction. In the simultaneous HDN/HDS reaction the presence of HDS had a strong inhibiting effect on HDN. This is caused by the competitive relation of the two reactions [39,43,44] and the fact that the presence of sulfur generates Ni_3S_2 which is not very active while hydrotreating and displays low activity during hydrogenation [45].

Results of elemental analysis CHNS and measurements of CO chemisorption after reactions indicate, that the main factor responsible for the decrease of the catalyst activity is formation of Ni_3S_2. The quantity of sulfur is three times higher that the quantity of carbon (for catalyst after HDN/HDS reaction)– Table 1. On the other hand, the analysis of the content of carbon in catalyst after the HDN alone reaction indicates that its quantity is 5 times higher (4.4%(HDN) vs. 0.85%(HDN/HDS). Despite of this, the catalyst in alone HDN reaction was much more active than in HDN/HDS reaction (Fig. 11). This indicates, that the main contribution to decreased activity of catalyst is sulphur - formation of Ni_3S_2 (very low activity).

Thus, when it forms, the amount of the metallic and boride active phase decreases, which leads to lowering of the catalyst activity. However, when Figs. 12 and 13 are compared in terms of the longest contact times–not the same (100% of HDN), the number of BCH isomers is dominant for the HDN/HDS reaction, which has been mentioned before. Although Ni_3S_2 is not very active during hydrogenation, according to the research by Daudin et al. [45] it was the most active in isomerisation of 2,3-dimethylbut-2-ene into 2-methylpentane of all examined sulfides Ni, Co, Fe, Pd, Pt, Rh, Mo, Ru. In this case, this could affect dominance of the BCH consecutive isomerisation. What is more, the presence of metal and acidic centres on the catalyst surface results in an increased isomeric activity, since bifunctional mechanism is allowed here [46]. In this case an increase of the number of BCH isomers was observed (the amount of EBC[4.4.0]decane and C_6CH higher than BCH). Therefore, the BCH consecutive isomerisation was the prevalent reaction during the simultaneous HDN/HDS reaction. Measurements of acidity (TPD of ammonia–7.95 μmol/g for HDN, 5.48 μmol/g for HDN/HDS) showed the presence of acidic centres either after carbazole HDN alone or simultaneous HDN/HDS reaction. The acidic centres were of rather medium and low strength [47]. Based on our studies on HDN of carbazole and literature [48–51] network of HDN of

carbazole was proposed (see Scheme 1). Three main hydrocarbons were detected: BCH, C_6CH and EBC[4.4.0]decane and also relatively small amount of CHB. The isomerisation as a consecutive reaction of BCH results in formation of C_6CH and EBC[4.4.0]decane, this occurs in both metallic and acid (specially Brönsted) centers. The Brönsted acid sides are formed (also "in situ") during the dissociative adsorption of H_2S (product of HDS reaction) to Ni by (abstraction of H from H_2S) forming SH species [52]. SH species may be also formed by dissociative adsorption of H_2S to Ni_3S_2 phase [53].

Therefore, catalyst 'modification' unavoidable in simultaneous HDN/HDS reaction and caused by partial sulfidation (forming of Ni_3S_2) affected lowered HDN activity of the catalyst and increased isomerisation activity under the HDN/HDS conditions applied.

Thus, the conditions applied for the HDS process have not led to complete sulfidation of the sample. In this case in applied conditions is possible keep our catalyst in partially metallic state. Similar results have been obtained by Bezverkhyy et al. [54] when studying the interaction between thiophene and Ni/SiO_2. The authors suggested that the interaction between thiophene and the catalyst was not direct. According to their suggestion, first, thiophene (here 4,6-DMDBT) is subjected to the desulfurization reaction and then the resultant H_2S reacts with Ni (NiB). In the applied conditions partial pressure of the resultant H_2S may reach equilibrium values for the Ni/Ni_3S_2 system. When S-compounds act as the source of sulfur, the catalytic reaction brings up two additional factors: (i) change the conversion of S-compounds (change the contact time–the space velocity) and therefore change the partial pressure of H_2S, (ii) on sulfidation the catalytic activity of a metal can provoke the change of H_2S partial pressure. In our case the ratio P_{H_2S}/P_{H_2} was in range from 3.1×10^{-4} to 6.2×10^{-6}. This ratio depends to conversion of DBT (in our case 4,6-DMDBT) and contact time of HDS reaction (flow of feed and H_2). In such case sulfidation is not complete [54]. In the HDS atmosphere involving the presence of H_2 and H_2S in gas phase in chemical equilibrium with the sulfide particles, sulfide particles should be reduced according to the reaction [55]:

$$Ni_3S_2 + xH_2 \leftrightarrow Ni_3S_{2-x} + xH_2S$$

In other site the reduction of bulk Ni_3S_2 into metallic nickel may take place as the lowest limit of sulfur chemical potential according to the chemical equilibrium [55]:

$$Ni_3S_2 + 2H_2 \leftrightarrow Ni + 2H_2S$$

So, Ni_3S_2 is not stable for P_{H_2S}/P_{H_2} ratio is lower than 10^{-5} [55]. As mentioned above for our case the ratio of P_{H_2S}/P_{H_2} was in range from 3.1×10^{-4} to 6.2×10^{-6}. For the temperature of reaction (350 °C) the equilibrium value P_{H_2S}/P_{H_2} is equal 2.51×10^{-5} [56].

It means, that Ni is the least resistance for the presence of sulfur (H_2S), because of thermodynamic equilibrium between metal and metal sulfide [57,58]. However, the tolerance for sulfur (the equilibrium) depends on the reaction temperature, ratio of H_2/feed, hydrogen pressure – globally from the hydrotreating conditions [57], but also on resistance for sulfur (because of boron) [8–10,59] and properties of catalyst.

On the basis of the XPS results obtained for amorphous boron alloy [9] it has been commonly accepted that boron gives some of its electrons to the nickel in the melt. The specific evidence leading to this conclusion was the difference in the bond energy of the elementary boron molten with nickel and pure boron [9]. Some of the boron electrons occupy the partly empty nickel orbital *d*, which makes boron electro-deficit, while nickel is electron-enriched. As a result, boron shows greater affinity to free electron pairs of e.g. sulfur or oxygen than nickel and protects the metal from sulfur poisoning or oxidation. On the other hand, the electron-enriched nickel shows affinity to unsaturated bonds, so it becomes active in hydrogenation reactions [9]. Moreover, the coordination number of the Ni—Ni bond is much higher than that of the Ni—B bond. It means that the content of nickel in the NiB alloy is much greater than that of boron. Additionally, the atomic mass of nickel is a few times greater than that of boron, so the energy of nickel bond is not so sensitive to changes as that of the boron bond [9].

Luo et al. [8] studied theoretically the adsorption of sulfur by the density functional theory calculations. According to their results, sulfur prefers bonding to boron and not to nickel in the alloy NiB alloys catalysts, which leads to protection of the active nickel from deactivation by sulfur in the catalytic reactions of hydrogenation. The results of Luo et al. [8] are fully consistent with those reported earlier by Li et al. [9] and have been confirmed by those of Wang et al. [10], who postulated that in NiB alloys sulfur is reversibly adsorbed on elementary boron.

Therefore we can say, that two factors play main role in incomplete sulfidation of catalyst in applied conditions: (i) resistance properties of NiB alloy for poisoning by sulfur, (ii) conditions of HDS reaction influence on thermodynamic equilibrium Ni/Ni_3S_2 system. In this way in applied HDN/HDS conditions is possible keep catalyst in partially metallic state. This allows to lead the process of HDN relatively fast on metallic phase Ni^0.

It appears that metallic active sites significantly affect activity of catalyst including noble metals during hydrogenation and hydrodenitrogenation of carbazole [42]. In this case, the bulk catalyst was very active in carbazole HDN alone, as mentioned before. Thus, the presence of Ni and/or Ni_3B determines activity of the preparation studied. The presence of boron influences an increased resistance of nickel (explains above), as an active phase against sulfur poisoning [8–10] during simultaneous HDN/HDS reaction, since both reactions proceed on the hydrogenation path on the same active sites [42].

The acidic centres are worth mentioning as well (or perhaps the acidic-metal balance of centres) which participate in hydrogenation and HDN reactions but, first of all, in isomerisation [60,61].

5. Conclusions

- Bulk NiB alloy is the precursor of true catalyst – bulk Ni^0 in environment of well dispersed boron species.
- Bulk catalyst was active in applied reaction – HDN of carbazole. Especially high activity the catalyst showed in alone HDN reaction in the whole range of applied contact times.
- The HDN reaction took place mainly on metallic phase – Ni^0.
- The main product of the HDN reaction (alone) was bicyclohexyl (BCH). It was also observed the consecutive reaction of isomerisation of the main product of the HDN reaction, BCH transformed into ethylbicyclo[4.4.0]decane (EBC[4.4.0]decane) and hexylcyclohexane (C_6CH).
- Opposite for HDN reaction with HDS the consecutive reaction of isomerisation of the main product of the HDN was dominant - BCH transformed first of all into EBC[4.4.0]decane.
- During alone HDN reaction observed decompositions of NiB on metallic Ni^0 and well dispersed boron.
- During the HDN/HDS reaction observed partially formed Ni_3S_2, metallic Ni^0 and Ni_3B phases. The activity was attributed mainly by presence of Ni^0 and/or Ni_3B phases.
- In applied conditions (HDN/HDS) is possible keep real catalyst in partially metallic state of Ni^0.

References

[1] W.J. Wang, H. Li, J.-F. Deng, J. Chem. Technol. Biotechnol. 75 (2000) 147–151.
[2] W.J. Wang, M.H. Qiao, H.X. Li, J.-F. Deng, Appl. Catal. A: Gen. 163 (1997) 101–109.
[3] X. Zhang, A. Ma, X. Mu, E. Min, Catal. Today 74 (2002) 77–84.

[4] S.T. Wong, J.F. Lee, J.M. Chen, C.Y. Mou, J. Mol. Catal. A: Chem. 165 (2001) 159–167.
[5] L. Wang, W. Li, M. Zhang, K. Tao, Appl. Catal. A: Gen. 259 (2004) 185–190.
[6] R. Zhang, F. Li, N. Hang, Q. Shi, Appl. Catal. A: Gen. 239 (2003) 17–23.
[7] M. Wang, F. Li, R. Zhang, Catal. Today 93–95 (2004) 603–606.
[8] C. Luo, W.N. Wang, M.H. Qiao, K.N. Fan, J. Mol. Catal. A: Chem. 184 (2002) 379–386.
[9] H. Li, H. Li, W.L. Dai, W. Wang, Z. Fang, J.-F. Deng, Appl. Surf. Sci. 152 (1999) 25–34.
[10] W.J. Wang, H.X. Li, J.-F. Deng, Appl. Catal. A: Gen. 203 (2000) 293–300.
[11] R. Prins, Adv. Catal. 46 (2001) 399–464.
[12] J.-F. Deng, H. Li, W. Wang, Catal.Today 51 (1999) 113–125.
[13] Z. Cheng, H. Abernathy, M. Liu, J. Phys. Chem. C: Lett. 111 (2007) 17997–18000.
[14] Y.Z. Chen, B.-J. Liaw, Sh-J. Chiang, Appl. Catal. A: Gen. 284 (2005) 97–104.
[15] G.L. Parks, M.L. Pease, A.W. Burns, K.A. Layman, M.E. Bussell, X. Wang, J. Hanson, J.A. Rodriquez, J. Catal. 246 (2007) 277–292.
[16] H. Li, Y. Wu, Y. Wan, J. Zhang, W. Dai, M. Qiao, Catal. Today 93–95 (2004) 493–503.
[17] M. Wang, H. Li, Y. Wu, J. Hang, Mater. Lett. 57 (2003) 2954–2964.
[18] H. Li, H. Li, J.-F. Deng, Mater. Lett. 50 (2001) 41–46.
[19] J.A. Schreifels, P.C. Maybury, W.E. Swartz, J. Catal. 65 (1980) 195–206.
[20] S. Diplas, J. Lehrmann, S. Jorgensen, T. Valand, J.F. Watts, J. Tafto, Surf. Interface Anal. 37 (2005) 459–465.
[21] N. Yu. Bekish, T.V. Gaevskaya, L.S. Tsybulskaya, Goo-Yul Lee, M. Kim, Prot. Met. Phys. Chem. 46 (2010) 325–331.
[22] W. Zhou, X.-J. Wu, X. Cao, X. Huang, Ch. Tan, J. Tian, H. Li, J. Wang, H. Zhang, Energy Environ. Sci. 6 (2013) 2921–2924.
[23] A.N. Buckley, R. Woods, J. Appl. Electrochem. 21 (1991) 575–582.
[24] B. Zhang, X. Ye, W. Dei, W. Hou, Y. Xie, Chem. Eur. J. 12 (2006) 2337–2342.
[25] Q. Wang, R. Gao, J. Li, Appl. Phys. Lett. 90 (2007), 143107(1)–143107(3).
[26] P. Marcus, J. Oudar, I. Olefjord, Mater. Sci. Eng. 42 (1980) 191–197.
[27] C.W. Oug, R.W.M. Kwok, Y.Y. Hui, W.M. Lau, J. Appl. Phys. 95 (7) (2004) 3527–3534.
[28] O.M. Moon, B.C. Kang, S.B. Lee, J.H. Boo, Thin Solid Films 464–465 (2004) 164–168.
[29] S. Kaciulis, Surf. Int. Anal. 44 (2012) 1155–1161.
[30] F.C. Tai, S.C. Lee, C.H. Wei, S.L. Tyan, Mater. Trans. 47 (2006) 1847–1852.
[31] Z.-B. Tu, M.-H. Qiao, H.-X. Li, J.-F. Deng, Appl. Catal. A: Gen. 163 (1997) 1–13.
[32] H. Li, H. Li, J.-F. Deng, Catal. Today 74 (2002) 53–63.
[33] H.H. Li, H.Y. Chen, S.Z. Dong, J.S. Yang, J.-F. Deng, Appl. Surf. Sci. 125 (1998) 115–119.
[34] S.E. Skrabalak, K.S. Suslick, Chem. Mater. 18 (2006) 3103–3107.
[35] S. Wei, H. Oyanagi, Z. Li, X. Zhang, W. Liu, S. Yin, X. Wang, Phys. Rev. B. 63 (2001) 224201–224205.
[36] A. Molnar, G.V. Smith, Bartok, Adv. Catal. 36 (1989) 329–383.
[37] M.V. Landau, Catal. Today 36 (1997) 393–429.
[38] I.I. Abu, K.J. Smith, Catal. Today 125 (2007) 248–255.
[39] M. Nagai, T. Masunaga, N. Hana-oka, Energy Fuels 2 (1988) 645–651.
[40] A. Szymańska, M. Lewandowski, C. Sayag, G. Djéga-Mariadassou, J. Catal. 218 (2003) 24–31.
[41] H. Ishii, M. Kiyoshi, M. Nagai, Top. Catal. 52 (2009) 1525–1534.
[42] M. Nagai, Y. Goto, A. Irisawa, S. Omi, J. Catal. 191 (2000) 128–137.
[43] G.C. Laredo, A. Montesinos, J.A. De los Reyes, Appl. Catal. A: Gen. 265 (2004) 171–183.
[44] P. Zeuthen, K.G. Knudsen, D.D. Whitehurst, Catal. Today 65 (2001) 307–314.
[45] A. Daudin, S. Brunet, G. Perot, P. Raybaud, C. Bouchy, J. Catal. 248 (2007) 111–119.
[46] C̈atalytic Naphtha Reforming", in: G.J. Antos, A.M. Aitani (Eds.), 2th ed., Marcel Dekker Inc, 2004, pp. 84–86.
[47] P. Berteau, B. Delmon, Catal. Today 5 (1989) 121–128.
[48] M. Nagai, H. Tominaga, D. Sugai, Chem. Lett. 42 (3) (2013) 272–274.
[49] A. Muto, T. Makabe, Y. Wada, T. Ono, Y. Shiroto, S. Inoue, J. Jpn. Petrol. Inst. 50 (6) (2007) 322–328.
[50] M. Nagai, T. Masunaga, Fuel 67 (1988) 771–774.
[51] D. Ferdous, A.K. Dalai, J. Adjaye, Energy Fuels 17 (2003) 164–171.
[52] D.R. Alfonso, Surf. Sci. 602 (2008) 2758–2768.
[53] N. Topsoe, H. Topsoe, J. Catal. 139 (1993) 641–651.
[54] I. Bezverkhyy, G. Gadacz, J.-P. Bellat, Mater. Chem. Phys. 114 (2009) 897–901.
[55] Y. Aray, A.B. Vidal, D.S. Coll, J. Rodriguez, D. Vega, J. Comput. Methods Sci. Eng. 9 (2009) 301–312.
[56] Xinjin Zhao, theses: Nickel deposition on hydrodemetallattion catalysts Massachusetts Institute of Technology, February (1993), page 35.
[57] Y. Yoshimura, M. Toba, T. Matsui, M. Harada, Y. Ichihashi, K.K. Bando, H. Yasuda, H. Ishihara, Y. Morita, T. Kameoka, Appl. Catal. A: Gen. 322 (2007) 152–171.
[58] A. Stoklosa, J. Stringer. Oxid. Met. 11 (1977) 277–288.
[59] W.J. Wang, M.H. Qiao, H.X. Li, W.L. Dai, J.-F. Deng, Appl. Catal. A: Gen. 168 (1998) 151–157.
[60] L.J. Simon, J.G. van Ommen, A. Jentys, J.A. Lercher, Catal. Today 73 (2002) 105–112.
[61] O. Cairon, K. Thomas, A. Chambellan, T. Chevreau, Appl. Catal. A: Gen. 238 (2003) 167–183.